 doi:10.20944/preprints202208.0002.v1

*Article*

# Analysis of A Piezo Stack Impact Actuation Mechanism for Freely Moveable Masses

**Matthias C Wapler , Constantin Peter, Koustav Kanjilal, and Ulrike Wallrabe**

IMTEK – Institute for Microsystems Technology, Albert-Ludwigs-Universität Freiburg;
Correspondence: wallrabe@imtek.uni-freiburg.de; Tel: +49 (0) 761203-7580

**Abstract:**

We present the prototype and analytical model of a miniaturized impact actuation mechanism, providing a fast out-of-plane displacement to accelerate objects against gravity, allowing for freely moving objects and hence for large displacements without the need of cantilevers. To achieve the necessary high speed, we chose a piezo electric stack actuator driven by a high-current pulse generator, connected to a rigid support and a rigid three-point contact with the object. We describe this mechanism with a spring-mass model and compare various inertial masses, all of them spheres, from different diameters and materials. As expected, we found that larger flight heights are achieved by harder projectiles, achieving, e.g., approx. 3 mm displacement for a 3 mm steel sphere using a 3x3x2 $mm^3$ piezo stack.

**Keywords:** piezo actuator; impact actuator; freely moveable masses

## 1. Introduction

Cantilever-type beams and springs replace bearings in the microscopic world because they are compatible with microsystem technologies and do not suffer from friction, which becomes large in relation to the other forces at small scales. When no force is applied, an object which is to be be moved or displaced is always in a defined neutral position, as the force of the actuator needed for the displacement is balanced by the restoring force of the bent cantilever. Cantilevers have hence the advantage of predictable forces, and positions and the absence of friction and wear with essentially no fatigue if made from silicon. The disadvantages are hardly discussed. These are exactly the opposite of what we stated before: The direction of motion is limited by the direction of force of the actuator, we always have to overcome the restoring forces by an actuator which does not only need to accelerate the object but also balance the force of the cantilever spring. The cantilever therefore limits the maximum displacement, and if we want to hold a displaced position we always have to provide force by the actuator, constantly consuming power.

Some impact microactuators have been investigated in the early years of MEMS, mostly to generate quasi-continuous motion without cantilevers, e.g. for rotation. Pisano et al. [1] and Muller et al. [2] were among the first to build impact based motors consisting of a comb actuators (suspended to cantilevers!) transferring its energy to a rotor assembled on a central hub.

In order to overcome the restrictions imposed by cantilevers, in this paper we present an impact "kick" actuation mechanism based on a piezoelectric chip actuator. The moving object, in this case a sphere, is not suspended on cantilevers or other springs, performing a free flight out of plane in one dimension according to gravitational acceleration. We investigated the acceleration of spheres of various diameters and materials, i.e. with different mass and hardness. The setup is characterized by measuring those trajectories and obtaining the initial kinetic energy or speed as a function of the mass of the object and the displacement of the actuator. We then relate these results to a mechanical spring-mass

Preprints (www.preprints.org) | NOT PEER-REVIEWED | Posted: 1 August 2022 doi:10.20944/preprints202208.0002.v1



model that takes into account the compliance of the actuator and the projectile and their masses.

## 2. Experimental Setup

For a demonstrator, we used a tiny PZT stack actuator (3 x 3 x 2 mm³, THORLABS PA3JEAW) with a fixed boundary condition at the bottom and an open boundary condition with three well-defined contact points for the projectile at the top. The projectile is then horizontally contained with a guidance structure that is supposed to guide the projectile back to the piezo in case it is released at an angle, but not to guide the projectile in normal direction. We drove the piezo with a low-impedance pulse generator in order to achieve fast speeds.

### *2.1 Mechanical and electric setup*

The mechanical set-up is shown in Fig. 1(a). As a base, we used a 10 mm block of aluminum into which we glued a 10x10 mm sheet of 1 mm thick glass to provide a smooth surface and spread the load of the piezo, which we glued with low-viscosity epoxy (Araldite 2020) at the center. To provide contact to the projectile, we used three 1 mm spheres of Zirconia. We glued them, again using Araldite 2020, in 1.1 mm holes with a 60° conical bottom and 1.35 mm pitch in a 1 mm thick titanium structure. To prevent the projectile from falling out of the experimental set-up, we created a guidance-structure that we laser-structured from 1 mm and 0.5 mm FR2 for the structural parts and 0.2 mm glass for the vertical guidance, leaving 0.125 mm space next to the projectile. We designed the structure to fix all its degrees of freedom when fitted together and fixated the pieces with cyanoacrylate "superglue"; it rests in a circular grove in the aluminum base.

To achieve a fast response time of the piezo, we needed a voltage source with a high peak current. For that purpose, we used the circuit shown in Figure 1(b), where we stabilized the input voltage with a 2.2 µF capacitor $C_{src}$ and applied it with an N-channel MOSFET (FQP32N20C) to the 113 nF piezo ($C_{PZT}$).

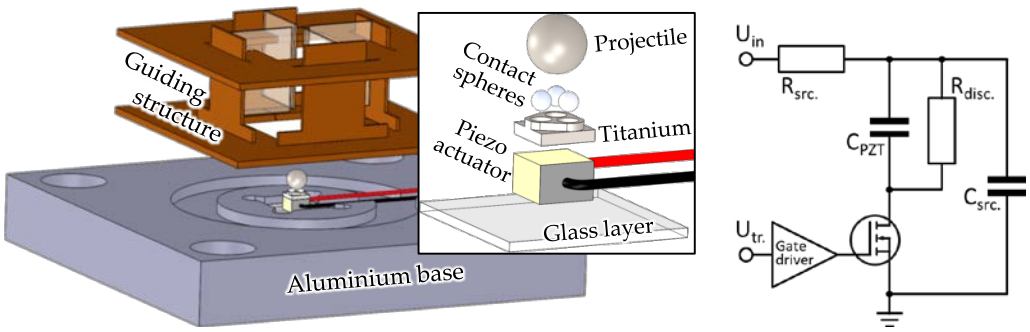


**(a)** **(b)**

**Figure 1.** (**a**) Exploded view of the experimental setup. **(b)** Electric driving circuit.

### *2.2 Setup characterization*

We characterized both the actuator and the flight trajectories of the projectiles with optical sensors, in both cases taking a number of samples ($21^2$ to $41^2$) over an area of 200 x 200 µm. For the characterization actuator, we used a Keyence LK-H022K triangulation sensor that we operated at a sampling frequency of 200 kHz. In Figure 2, we show the mechanical and electrical response at 100 V input voltage. We see a fast mechanical response of approx. 10 µs, followed by a superposition of different resonances and a long-term creep. The height of the displacement should not be considered as an exact value as it may be different at different positions on the surface. Due to the noise even with a large number of samples, it is difficult to compute an accurate value of the initial speed of the piezo surface. Taking samples at 20 V and 100 V, we find a maximum speed of approx.

Preprints (www.preprints.org) | NOT PEER-REVIEWED | Posted: 1 August 2022 doi:10.20944/preprints202208.0002.v1



100 to 130 $ms^{-1}$ times the asymptotic displacement at the given voltage, which corresponds well to the response time. We also see that the electric response of the circuit is sufficiently fast in order not to affect the mechanical response. The difference of about 5% of the initial value compared to the input voltage can be explained by the ratio of the capacitances. We verified that the actuator is not limited by its internal resistance or inductance by measuring the impedance spectrum, which showed the typical resonance (480 kHz) and anti-resonance (600 kHz) in addition to a few highly suppressed modes that may result from the aluminum base. At the frequency range of relevance for the step response between 10 and 100 kHz, the actuator acts like a near perfect capacitor with 104 nF and a phase between -89.2° and -89°. Between 20 and 24 kHz, there is a very small fluctuation in the phase of about 0.05°, and another one between 45 and 70 kHz with 0.15°, which may correspond to the mechanical ringing that we see in the step response in Fig. 2.

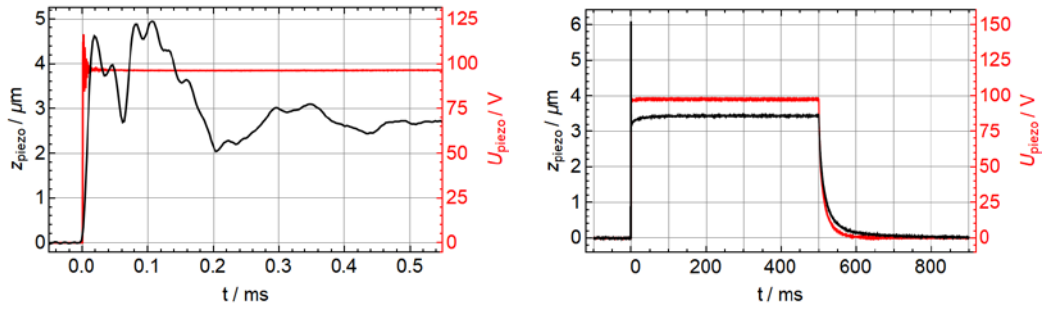


**Figure 2**. Displacement of the surface of the actuator setup (black) and electric signal (red) for a trigger signal of 1 Hz and 50% duty cycle and an input voltage of 100 V, initial response (left) and full cycle (right).

To demonstrate the kinematics, we show the trajectory of a 3 mm 1.4034 hardened steel ball in Figure 3 that we measured with a chromatic confocal sensor (Polytec CL4). We see the usual kinematics with approximately constant total energy and a series of bounces of the projectile on the piezo actuator. One has to keep in mind that the speed is comparatively noisy, and there may be contact with the guidance structure and a possible rotation of the projectile, in particular after the bounces. We did not track the actual spherical shape of the surface, so there may be some artefacts coming from a sideways motion in combination with the spherical surface profile that appear as an altered overall speed in combination with a slightly stronger gravitational acceleration. With a speed of at most approximately 0.2 m/s, we ignore aerodynamic friction for the rest of the paper.

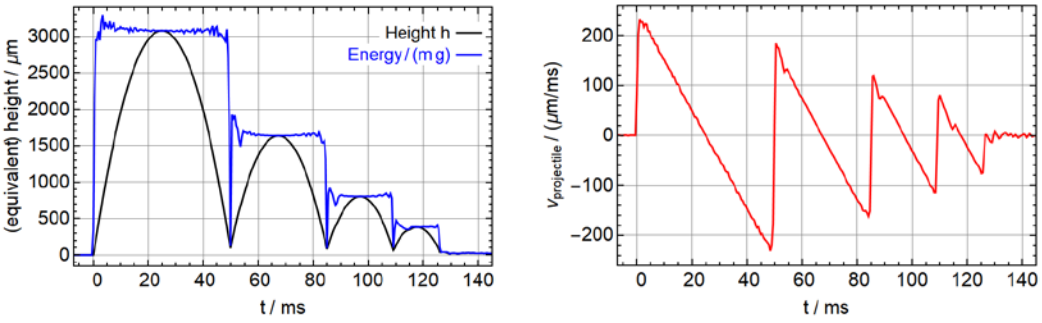


**(a)** **(b)**

**Figure 3.** Single kick of a 3 mm hardened steel sphere, ejected at 100 V input voltage. (a) Vertical position and total computed energy (linear kinetic plus potential). (b) Vertical speed.

*2.3 Mechanical model*

To first order, such a device can be described by a simple spring-mass model with an effective spring constant $\boldsymbol{k_{eff}}$ representing the stiffness of the actuator assembly and

Preprints (www.preprints.org) | NOT PEER-REVIEWED | Posted: 1 August 2022 doi:10.20944/preprints202208.0002.v1



possibly a section of the projectile, and a mass $M = m_{eff} + m$ consisting of an effective mass $m_{eff}$ of the actuator setup and the mass $m$ of the projectile. In Fig. 4, we illustrate that immediately after applying the electric signal, the spring is in a compressed state corresponding to the total DC displacement $z_0$ (ignoring creep effects). It then relaxes with a harmonic motion with an angular frequency $\omega = \sqrt{k_{eff}/M}$, starting the projectile at the maximum speed $v = \omega z_0$. Hence, we expect a linear dependence of the initial speed of the projectile on the DC displacement of the actuator for different input voltages. The angular frequency should increase with decreasing mass, approaching the 100 to 130 $ms^{-1}$ of the bare actuator setup at zero mass, even though $m_{eff}$ and $k_{eff}$ will depend on the mechanics of the actuator-projectile contact, i.e., on the size of the projectile and its hardness.

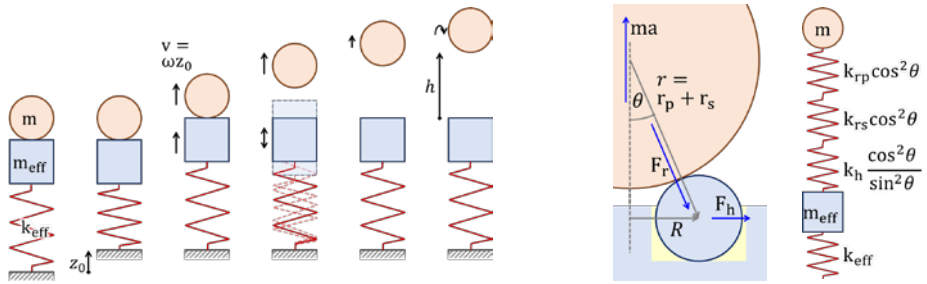


**Figure 4.** (a) Spring-mass model of the acceleration process. (b) Detailed model of the contact point between projectile and contact spheres. (c) Detailed spring-mass model.

We can describe those details to some approximation by introducing an additional spring constant $k_{contact}$ that describes the contact between the actuator assembly and the projectile. To obtain this spring constant, we assumed that the acceleration of the projectile is balanced by a force that is orthogonal to the surface at all three contact points, resulting in a horizontal force of the contact spheres acting on their titanium mount, and the glue as shown in Fig. 4 (b) and (c). In terms of the spring constants $k_h$ describing the horizontal deformation or displacement of the spheres and $k_{rs}$ and $k_{rp}$ describing the deformation of the spheres of the projectile, $k_{contact}$ becomes then

$$\frac{1}{k_{contact}} = \frac{3}{\cos^2\theta}\left(\frac{1}{k_{rp}} + \frac{1}{k_{rs}}\right) + \frac{\sin^2\theta}{\cos^2\theta}\frac{3}{k_h} \,. \quad (1)$$

Splitting the deformation of the spheres and the projectile allows us to take into account the different deformations of the projectiles, assuming, e.g., proportionality to the hardness of the material. We then further assume that the initial speed of the projectile is described by the slowest in-phase mode of the combined spring-mass system,

$$\omega^2 = \frac{k_{contact}m_{eff} + k_{eff}(m + m_{eff}) - \sqrt{\left(k_{contact}m_{eff} + k_{eff}(m + m_{eff})\right)^2 - 4k_{eff}k_{contact}m\,m_{eff}}}{2m\,m_{eff}} \,. \quad (2)$$

## 4. Measurements and Discussion

We demonstrated our setup using spherical projectiles of tungsten carbide, zirconia and hardened and non-hardened stainless steel, summarized in Table 1, with diameters 3, 4 and 5 mm.

**Table 1.** Summary of the materials.

| Material | Density [1] | Y-modulus | Hardness |
|---|---|---|---|
| Zirconia ($ZrO_2$) | 6090 kg/m³ | 205 GPa[4] | 1200-1400 HV[2], 78 HRC[3] |
| 1.4034 hardened steel | 7710 kg/m³ | 215 GPa[5] | 54-60 HRC[2], 60 HRC[3] |
| 1.4401 untreated steel | 7990 kg/m³ | 200 GPa[6] | 25-39 HRC[2,3] |

Preprints (www.preprints.org) | NOT PEER-REVIEWED | Posted: 1 August 2022 doi:10.20944/preprints202208.0002.v1



| | | | |
|---|---|---|---|
| Tungsten carbide TC2 | 14800 kg/m[3] | 669-696 GPa[7] | 1400-1500 HV[2], 78 HRC[3] |

[1] Measured, [2] Supplier data [3], [3] Supplier data [4], [4] Supplier data [5], [5] Supplier data [6], [6] Supplier data [7], [7] Supplier data [8]

*4.1 Measurement protocol*

We measured the acceleration each projectile over a sequence of input voltages from 20 to 100 V. For each combination, we measured a total of 441 events with a continuous trigger of 1 Hz on a 21x21 grid on 200 x 200 µm around the center of the projectile, again using the CL4 chromatic confocal sensor at a sampling rate of 2 kHz. To exclude effects from friction on the sidewalls of the guidance structure, rotation of the projectile or improper contact with the actuator assembly, we placed several filters on the data of each shot, excluding data with:

- > 0.5 ms deviation of the actual flight time from the expected flight time obtained from the maximum height
- > 1% or 2 µm/ms deviation of the initial speed from kinematic expectation
- > 4% deviation from the gravitational acceleration or
- a horizontal speed (obtained from the measured acceleration and sphere diameter) greater than 20 µm/ms or 15% of the vertical speed.

To be more robust against possible further errors, we then took the median value rather than the mean value of the remaining measurements. Our results hence do not conclude on how well all movements follow Newtonian kinematics, but they give the results of the median flight height for those that appeared to have a sufficiently vertical flight path with standard kinematics without friction.

To reference the flight height or the resulting initial speed to the piezo displacement, we measured the near-asymptotic displacement of the actuator as a function of the voltage. As in section 2.2, we used our LK-H022K triangulation sensor, now at 20 kHz which is less noisy than the 200 kHz and only on an 8 x 8 grid over 200 x 200 µm. As it was difficult to measure on the ceramics spheres, we measured near the edge of the titanium plate, which may have a slightly different overall displacement. Using the same 1 Hz actuation frequency as for the acceleration of the spheres, we used averages over each the last half of the rest state and displaced state to obtain the displacement. Finally, we fitted a 4$^{th}$ order polynomial (without constant) into the voltage dependent displacement.

*4.1 Measurement results*

In fig. 5 (a), we show the median initial speed of the different projectiles as a function of the piezo step height, obtained from the maximum flight height as measuring the speed is comparatively noisy. We find a very linear dependence of the initial velocity on the piezo displacement, as we expect from the spring-mass model, with slower velocities for the heavier projectiles. In particular for the smaller projectiles, we could not obtain data at all voltages, as for high voltages, some exceeded the measurements range of the sensor and the measurements became overall less reliable, probably due to a higher likelihood of friction with the guidance structure. In fig. 5 (b), we show the corresponding angular velocity as a function of the projectile mass for the different materials. As expected, we see a decreasing angular frequency with increasing mass and a convergence roughly towards the regime of the angular frequency that we measured for the unloaded actuator assembly in section 2.2.

Preprints (www.preprints.org) | NOT PEER-REVIEWED | Posted: 1 August 2022 doi:10.20944/preprints202208.0002.v1



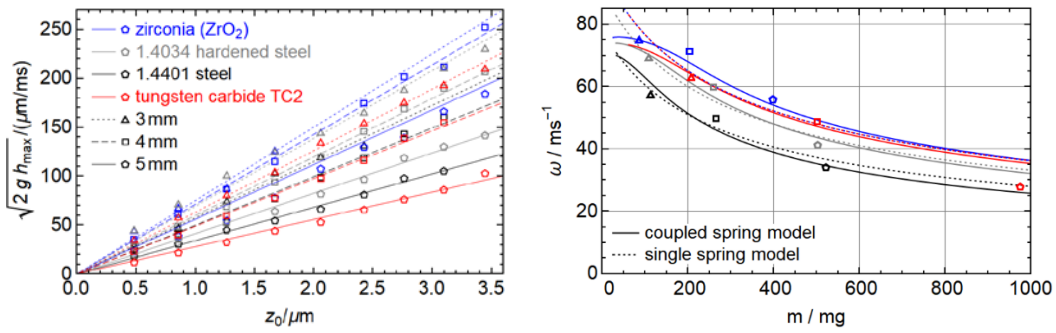


(a) (b)

**Figure 5.** (a) Initial speed of the different projectiles as a function of the displacement of the piezo actuator. (b) Corresponding angular frequency of the spring-mass model as a function of the projectile mass.

Fitting our model from equations (1) and (2) to the data gives a reasonably good description of the behavior, but still some deviations. It turned out that taking $k_{rp}$ in the model proportional to the hardness resembles the data much better than using the Young's modulus. There is, however little difference of which of the hardness values we use in the range in Table 1, and whether we use the given HRC values or the HV values (and convert the values for the steel projectiles). Also small modifications to the geometric model do not change the quality of the fit. One also has to take into account, however, that this is a 5 parameter model fitted to just 9 measurement values. Yet, the qualitative fit turns out to be much better than the simple spring-mass system with just $\boldsymbol{\omega} = \sqrt{\boldsymbol{k_{eff}}/(\boldsymbol{m} + \boldsymbol{m_{eff}})}$, even if we introduce an additional linear dependence of $\boldsymbol{m_{eff}}$ and $\boldsymbol{1/k_{eff}}$ on both the hardness. Our fit predicts a rather low effective mass of just 16 mg and effective spring constant of 0.11 N/µm compared to the mass of just the piezo of approx. 200 mg and 200 N/µm (typical values, [4]). Yet, those values correspond to a resonance frequency around 80 kHz, not far from the 100 to 130 kHz of the bare actuator assembly, so they are consistent and suggest that most of the deformation takes place near the top of the assembly. The value of $k_h$ is ~~o~~ 0.27 or 0.33 N/µm depending on which hardness values we use, which makes sense given that the spheres are horizontally fixated by a glue layer. $k_{rs}$ and $k_{rp}$ combine to between 0.24 and 0.49 or 0.51 N/µm for the different materials.

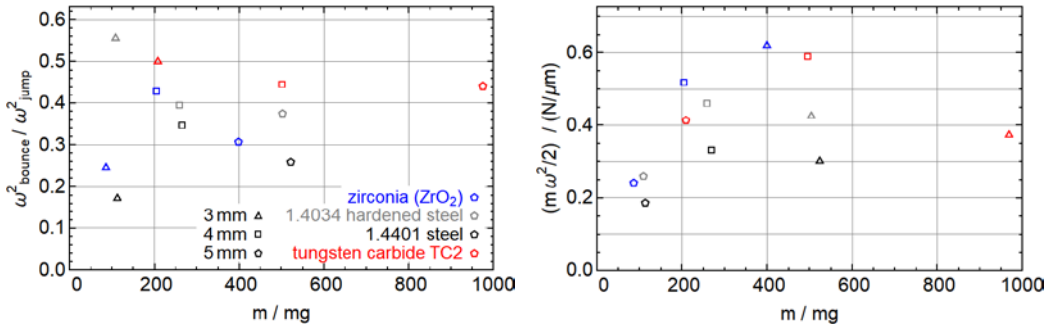


(a) (b)

**Figure 6. Left: Fraction of energy recovered in the first bounce for different objects. Right: Ratio** of initial kinetic energy to the actuator displacement, which is, in an ideal simple spring-mass mode the spring constant.

In Fig. 6 (a), we show the quality factor of the first bounce of the projectile, i.e., the ratio of the projectile energy in the initial acceleration phase and in the first bounce obtained from the fit parameter $\boldsymbol{\omega}$. While the data is not perfect, we find that the harder materials tend to have a better recovery of the energy, but metals (hardened steel and tungsten carbide) preserve more energy than the ceramic projectiles.

 doi:10.20944/preprints202208.0002.v1



To finally demonstrate how effectively our setup uses the possible strength of the actuator, we look in Fig. 6 (b) at the ratio of the energy of the projectiles to the square of the actuator displacement, given by $\frac{1}{2}m\omega^2$. We see that the highest value is achieved for the 5 mm zirconia and 4 mm tungsten carbide projectiles, with about 0.6 N/µm. Comparing this to the energy $\frac{1}{2}k$ that can be stored in a spring, we find that this value is, on the one hand, much larger than the fitted value for $k_{eff}$ , casting a little doubt on our spring-mass system. On the other hand, it is still much smaller than the spring constant of a bare piezo, suggesting that our setup is not the most effective way to accelerate a projectile with a piezo actuator.

## 5. Conclusions

We have demonstrated a ballistic actuator based on a 3 x 3 x 2 mm³ piezo stack actuator, accelerating projectiles with 3 to 5 mm diameter and different materials: untreated and hardened steel, ceramics (zirconia) and hard metal (tungsten carbide). To avoid effects due to uneven surfaces or dirt particles, we designed a contact structure consisting of three 1 mm zirconia spheres, mounted in a thin titanium structure. We found that this system can be reasonably well described by a spring-mass system describing the spring and mass of the lower part of the actuator assembly coupled to a spring of just the contact points and the mass of the projectile. According to our model, most of the elastic deformation takes place in the upper actuator assembly. This stresses that the design and fabrication of a contact structure that provides a well-defined contact but at the same time as little deformation as possible is the key to achieve a large momentum transfer to the projectile. Obviously, the height of the trajectories was larger, the lighter and harder the projectile; with the smallest zirconia spheres, we exceeded the 4 mm range of our measurement sensor.

The highest energy of the projectile per actuator displacement-squared was approx. 0.6 N/µm, a factor of 130 smaller than what could be achieved with an ideal piezo actuator. Our results demonstrate that using short stroke actuators may not be the most effective approach to piezo ballistic actuators. It may be a more sensible approach to use bending or buckling actuators such as [5, 6] that potentially accelerate the projectile with a slower but larger stroke and are hence less sensitive to deformations of the contact points.

**Supplementary Materials:** Not applicable.

**Author Contributions:** MCW conceived the experiments and experimental setup, developed the model, analysed the measured data, and wrote the main part of the paper. CP performed the measurements, KK implemented the experimental set-up and partially contributed to figures. UW initiated the project, acquired funding, wrote the introduction. MCW and UW co-supervised the students and the project.

**Funding:** This research was funded by the German Research Foundation (Deutsche Forschungsgemeinschaft - DFG) under grants WA 1657/10-1 and WA 4555/2-1.

**Data Availability Statement:** The data presented in this study are available on request from the corresponding author.

**Conflicts of Interest:** The authors declare no conflict of interest.

## References

1. Lee A P; Nikkel D J Jr; Pisano A P Polysilicon linear microvibromotors, Proc. 7th Int. Conf. Solid-State Sensors and Actuators **1993**, pp 46–9
2. Daneman M J; Tien N C; Solgaard O; Pisano A P; Lau K Y; Muller R S Linear microvibromotor for positioning optical components J. Microelectromech. Syst. **1996**, 5 159–65

 doi:10.20944/preprints202208.0002.v1




3. Supplier website, https://www.kugel-winnie.de/epages/62136757.sf/de_DE/?ObjectPath=/Shops/62136757/Categories/Kugeln (obtained 03/2022)
4. Supplier data sheets, https://www.kugel-winnie.de/epages/62136757.sf/de_DE/?ObjectPath=/Shops/62136757/Categories/Infos (obtained 05/2022)
5. Supplier website, https://www.syalons.com/materials/zirconia/ (obtained 06/2022)
6. Supplier website, https://virgamet.com/x46cr13-x40cr14-z44c14-x39cr13-x46crs13-s42080-stainless-steel (obtained 06/2022)
7. Supplier website, https://www.thyssenkrupp-materials.co.uk/stainless-steel-316-14401.html (obtained 06/2022)
8. Supplier website, https://www.matweb.com/search/DataSheet.aspx?MatGUID=e68b647b86104478a32012cbbd5ad3ea&ckck=1 (obtained 06/2022)
9. Bruno, B.P.; Fahmy, A.R..; Stürmer, M.; Wallrabe, U.; Wapler, M.C. Properties of piezoceramic materials in high electric field actuator applications. *Smart Materials and Structures* **2019**, *28*, 015029.
10. Wapler, M.C.; Brunne, J.; Wallrabe, U. A new dimension for piezo actuators: free-form out-of-plane displacement of single piezo layers, *Smart Mater. Struct*. **2013**, *22*, 102001
11. Wapler, M.C.; Stürmer, M.; Wallrabe, U. A Compact, Large-Aperture Tunable Lens with Adaptive Spherical Correction, In Proceedings of the 2014 International Symposium on Optomechatronic Technologies, Seattle, WA, USA, 5-7 Nov. 2014